November 2013

Contrast Adaptation in the Lateral Eye of *Limulus polyphemus*

Tchoudomira Valtcheva
University of South Florida, tvaltche@mail.usf.edu

Contrast Adaptation in the Lateral Eye of *Limulus polyphemus*

by

Tchoudomira Milkova Valtcheva

A thesis submitted in partial fulfillment
of the requirements for the degree of
Master of Science in Biomedical Engineering
Department of Chemical and Biomedical Engineering
College of Engineering
University of South Florida

Major Professor: Christopher Passaglia, Ph.D.
Robert Frisina, Ph.D.
Joseph Walton, Ph.D.

Date of Approval:
November 1, 2013

Keywords: retina, ommatidia, sensitivity,
optic nerve, luminance

DEDICATION

I dedicate the work I have completed in my journey as a student to my parents, Milko and Maria, and to my sister, Iva. They believed in me when I didn’t believe in myself and I would not be where I am today without their unconditional love and support.

ACKNOWLEDGMENTS

I first and foremost express my immense gratitude to Dr. Christopher Passaglia for allowing me the opportunity to work with him on this project. His exceptional sponsorship and guidance has made this degree possible and I feel optimistic and prepared to enter the professional world as a Biomedical Engineer because of the countless invaluable lessons I have learned while working with him. I will truly cherish my time spent at the lab, even though there were often times when I thought for certain my sanity would leave and never come back.

I want to sincerely thank my defense committee, Drs. Frisina and Walton. I appreciate the time they have spent with me and their and supervision and guidance in completing this important chapter in my life.

I would like to give a special recognition to Dr. Venkat Bhethanabotla and Sebnem Thiel for their help with my acceptance and successful completion of my Master's degree here at the University of South Florida.

TABLE OF CONTENTS

LIST OF TABLES

LIST OF FIGURES

ABSTRACT

Luminance and contrast adaptation are neuronal mechanisms that the retina applies for continuous adjustment to light sensitivity though a collection of cellular and synaptic mechanisms distributed across the retinal network, thus accommodating the wide input range of the visual system within the constricted output range of retinal ganglion cells. Luminance mean adaptation has been demonstrated in the output neurons of the invertebrate eye (eccentric cells), and the aim of the study was to investigate whether the homology in visual processing extends to luminance variance (contrast) adaptation as well. The spike trains of individual eccentric cells were recorded from live horseshoe crabs to white noise stimuli of varying contrast delivered to optically-isolated ommatidial receptors. Linear-nonlinear models estimated from the spike output of eccentric cells decreased in gain with increasing contrast of white noise, suggesting an unknown mechanism of contrast adaptation may operate in the retina. Given the simple organization of the horseshoe crab eye determining whether this mechanism exists in the retina is of fundamental importance to vision research.

CHAPTER 1: INTRODUCTION

1.1 Adaptive Processes in the Vertebrate Retina

The visual system is one of the numerous impressive wonders of nature and biology. It is a key sensory pathway for communication with the outside world and essential for survival. Vision is a means of information processing and esthetic enjoyment (Shapley and Enroth-Cugell, 1984). Neuroscientists and neuroengineers aim to understand and define the visual system, to improve disease detection, treatment and prevention as well as to aid in the development of ocular assisting devices for those whose eyes cannot be saved.

The role of the eye is to relate visual information about the environment to the brain. All of our visual experience derives from sequences of action potentials propagated from the retina through the optic nerve to the brain, illustrated in Figure 1.1.

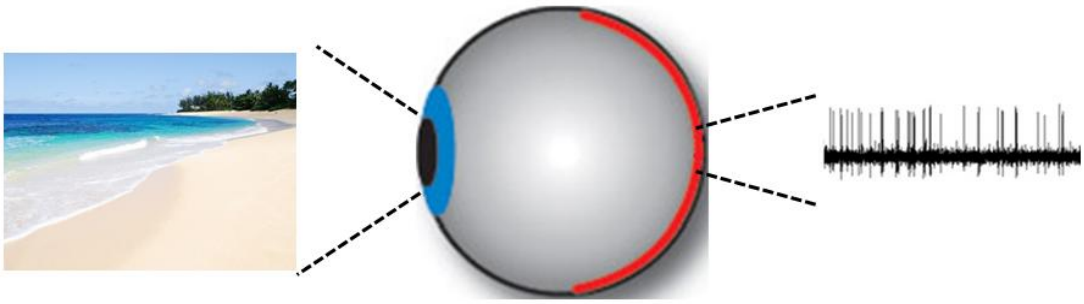

Figure 1.1 Visual Processing

The retina is among the most intensively studied systems in the vertebrate neural network. It is a light sensitive tissue layer in the back of the eye composed of seven main types of cells organized into three distinct layers, shown in Figure 1.2 (Dowling, 1987):

1. The outer nuclear layer (ONL) comprised of rod and cone photoreceptor cells.
2. The inner nuclear layer (INL), which includes the bipolar cells, horizontal cells, amacrine cells and Müller glial cells.
3. The ganglion cell layer (GCL) housing ganglion cells and displaced amacrine cells.

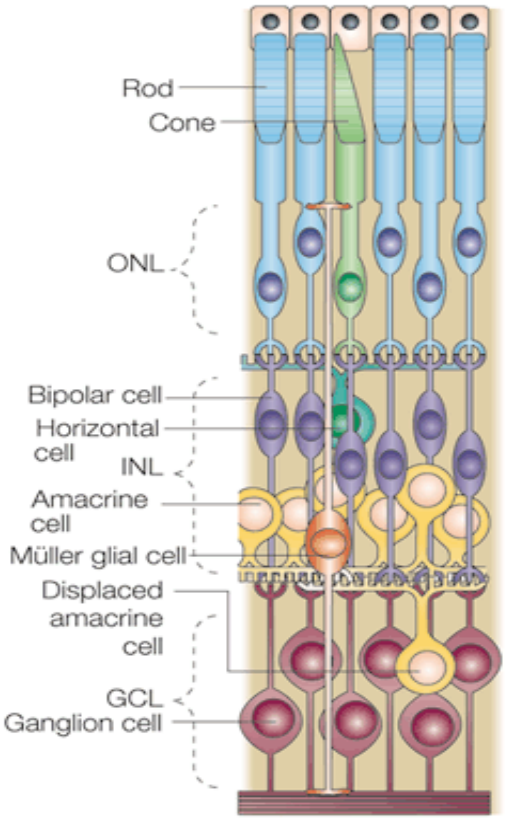

Figure 1.2 The Vertebrate Retina (Dyer and Cepko, 2001)

The optics of the eye, such as the lens and cornea, project the image we see from our world onto the retina. When light hits the retina, some cells are illuminated more brightly than others. The horizontal cells play an important role at this stage of visual processing. They are able to selectively inhibit the output of the less-illuminated regions, while leaving adjacent cells unaffected. This process is called lateral inhibition and it ensures that only highest-intensity signal is selected, improving visual definition. Lateral inhibition is an elaborate network seen at multiple levels in the visual system (Roska *et al.,* 2000). The photoreceptor cells then transmit the signal through the bipolar cells to the retinal ganglion cells, which produce action potentials propagated through the optic nerve to the brain. The retina must consistently adjust its sensitivity to visual stimuli in order to accommodate a wide stimulus input range within the limited output range of retinal ganglion cells. This process is called adaptation and it is one of the fundamental operations performed by the retina. The adaptation phenomenon decreases sensitivity when the stimulus is high to avoid response saturation, and increases sensation to low stimulus to improve signal-to-noise ratio. The "noise" is composed of various biological factors, such as physiological fluctuations in the retina and spontaneous firing of neurotransmitters in the brain (Shapley and Enroth-Cugell, 1984). Adaptation is an intricate and involved process that helps retain visual constancy in the brain via concerted feedback mechanisms and has been seen at several different levels within

the retinal network (i.e. photoreceptors, bipolar cells and amacrine cells). Luminance and contrast adaptation are two systems present in the retina that are used to retain visual steadiness in the event of a change in visual stimulus.

Luminance, or light, adaptation is a well-established mechanism across many animal species, including *Limulus polyphemus,* and it acts to adjust the dynamics of the retina as mean illumination level changes, retaining visual sensitivity (Gollisch and Meister,2010; Tranchina *et al.,*1984;Tamura *et al.,*1989;Purpura *et al.,*1990). It allows encoding and processing of visual information over a million-fold intensity range. The threshold intensity of cells decreases as their sensitivity increases with time spent in the dark, shown in Figure 1.3. It takes about 30 minutes for the retina to adapt to a dark environment. Rods are more sensitive to light and take longer to adapt.

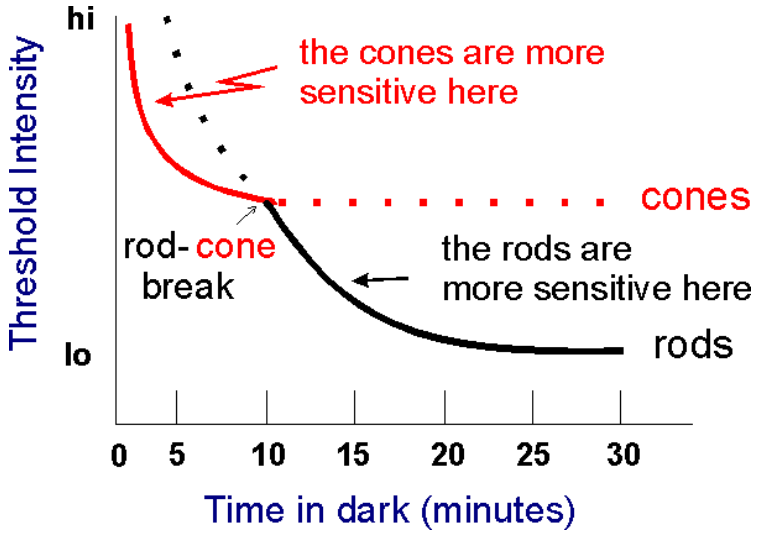

Figure 1.3 Light Adaptation (Perter Kaiser, 2013)

Contrast adaptation, or contrast gain control, is a more recent discovery and the focus of this study. It is adaptation to changes in the variance of light intensity about the mean illumination level, as illustrated in Figure 1.4A. Figure 1.4B is a representation of the cell response without any adaptation to change in stimulus intensity, where the cell membrane potential is modulated at a rate proportional to the stimulus input. At high levels of contrast the firing rate is saturated and distorted, leading to loss of information and inability to process the image accurately. Figure 1.4C shows the gain, or sensitivity, reduction followed by an increase in contrast as the cell adapts to a change in input, avoiding response saturation. The sensitivity is increased when the stimulus intensity is changed back to a low level, returning the system to its initial state.

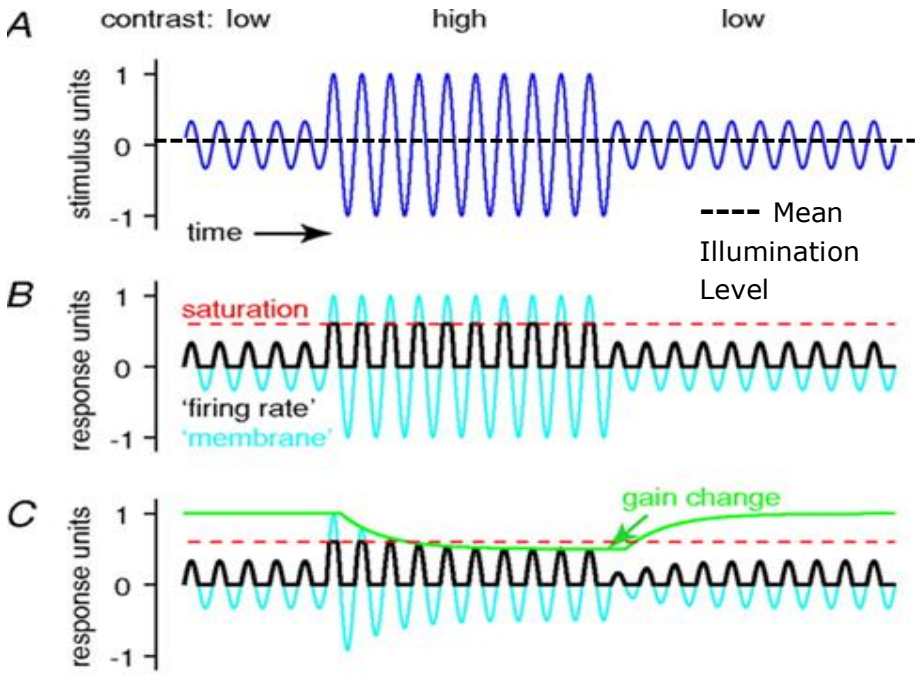

Figure 1.4 Contrast Adaptation (Demb, J. B., 2008)

Contrast adaptation has only been demonstrated in the vertebrate retina to date (Chandler and Chichilnisky, 2001; Zaghloul, Boahen and Demb, 2005; Demb, 2008). Mechanisms for contrast gain control are found in the presynaptic bipolar cell outputs as well as in the process of spike generation, suggesting the existence of multiple synaptic and intrinsic mechanisms for contrast adaptation in the visual processing cascade (Baccus and Meister, 2002; Zaghloul *et al*., 2007; Yu, Y. and Lee T.S., 2003).

The inference made in the literature is that luminance and contrast adaptation are modulated via disconnected gain control mechanisms (Green *et al.,*1977), however different models have not been fully evaluated. Defining these phenomena and their correlation is of fundamental importance to vision research.

1.2 The Horseshoe Crab in Vision Research

The visual system of the horseshoe crab has played an important role in vision research. *Limulus* processes visual information with excitatory and inhibitory mechanisms similar to those found in the vertebrate retina (Passaglia *et al.,*1997). By studying its neural network, scientists have been able to gain much insight about neurophysiological processes that may operate in the vertebrate eye, including light adaptation. The horseshoe crab provides a valuable testing structure for vision research due to its compact, easily accessible and well-defined visual system (Snodderly, 1971). It possesses the largest neural network for which a quantitative cell-based

model exists (Passaglia *et al.,* 1998). The *Limulus polyphemus* visual behavior is complex enough to be intriguing, yet simple enough to be understood and explained.

The location of the eyes of the horseshoe crab is shown in Figure 1.5. The horseshoe crab possesses a total of 10 light-receptive organs. It has median, rudimentary and endoparietal eyes all found on the top of the carapace. *Limulus polyphemus* has two ventral eyes located on the underside near the mouth and light sensors along its tail. These eyes help the crab with navigation and light sensation. The median eyes have the capability to detect both visible and UV light and aid in following the lunar cycle, which is essential for spawning (Wald and Krainin, 1963). The two large, bean-shaped structures on the carapace are the lateral compound eyes, the only eyes that subserve pattern vision (Barlow *et al*., 1982). The compound eyes are primarily used for mating and are the focus of vision research and this project. They are made up of roughly 1,000 ommatidial units about 140 μm in diameter, shown in Figure 1.6. They exhibit many functional characteristics analogous to those found in the vertebrate retina. The structure of the *Limulus* ommatidia is shown in Figure 1.7.The anatomy is much simpler compared to the vertebrate eye. Transformation of light patterns into trains of impulses originating in the eccentric cells is the first stage of visual processing (Passaglia *et al.,* 1997).

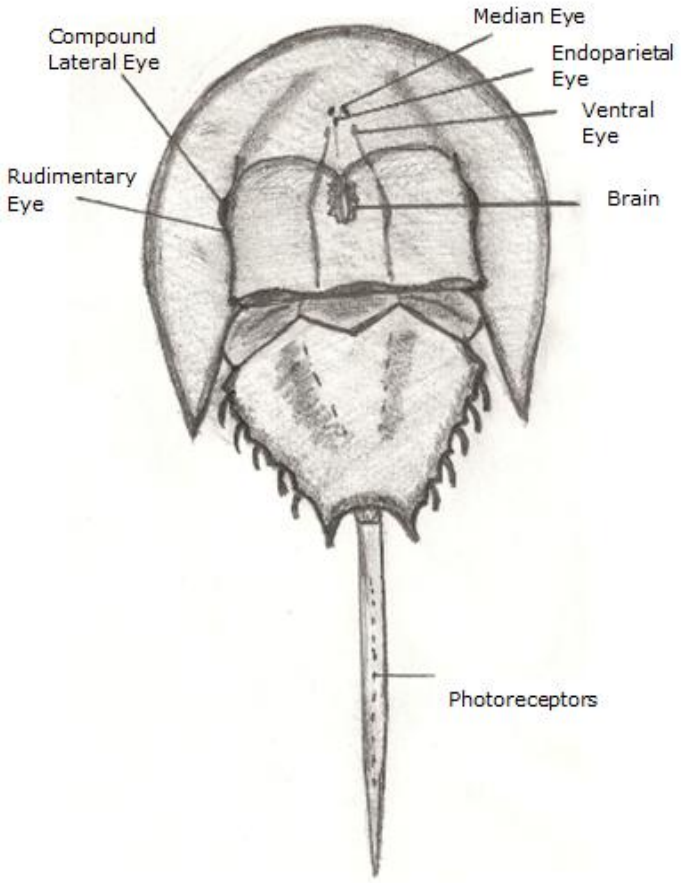

Figure 1.5 The Visual System of the Horseshoe Crab

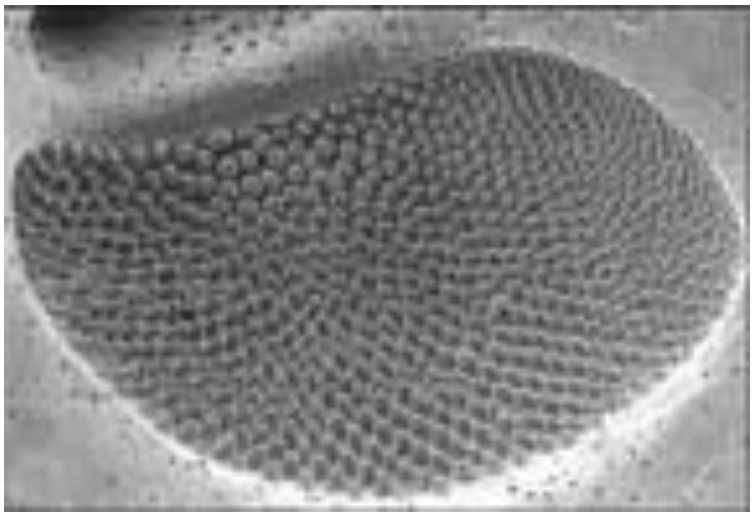

Figure 1.6 Lateral Compound Eye (ERDG. Retrieved on 10/10/2013)

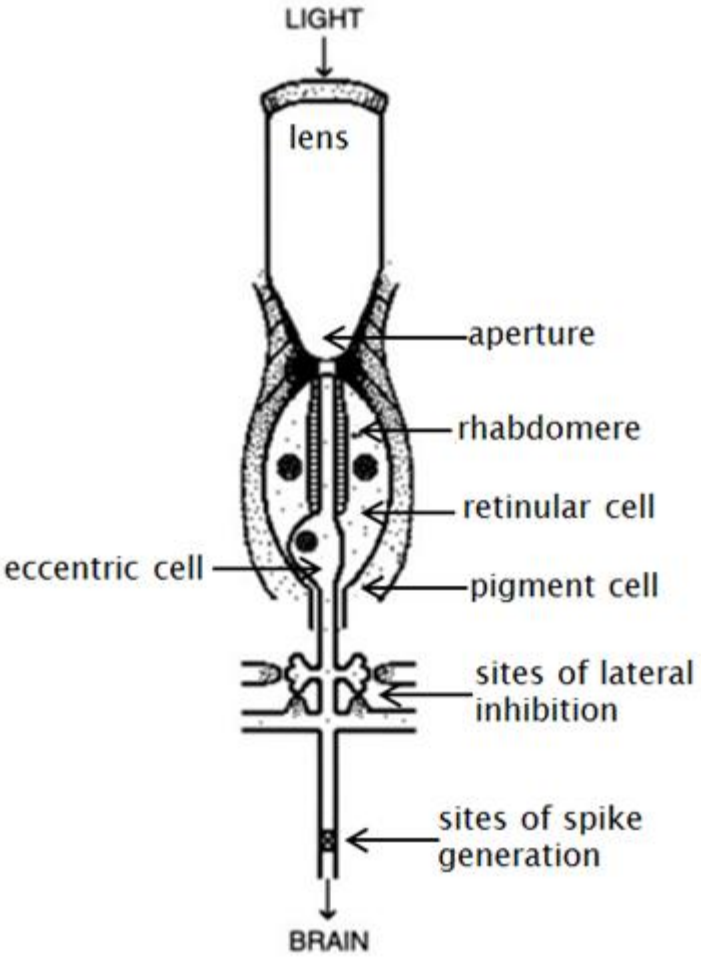

Figure 1.7 Ommatidial Structure (Passaglia *et al.,* 1997)

Each corneal unit has a lens that collects and focuses light from about a 6^{o}-12^{o} aperture formed by the process of pigment cells onto the photosensitive rhabdomeres of 10-12 retinular cells. That signal is then sent to the eccentric cells in the form of a photocurrent, which produce action potentials propagated through the optic nerve to the brain. The cascade "remembers" past visual stimuli and adjusts the properties of the eye accordingly. The optic nerve is resilient and easily reachable, which provides a straightforward way to record and analyze the electrical signals the eye

sends to the brain. Both lateral and self-inhibitory mechanisms have been demonstrated in the eccentric cells of the horseshoe crab (Hartline *et al*., 1961; Stevens, 1964; Purple, 1964; Purple and Dodge, 1966). The horseshoe crab is an excellent research model and the one chosen for this study. Contrast adaptation has not been demonstrated in the invertebrate eye, though a similar mechanism has been reported in the post retinal circuitry (Laughlin, 1989; Green, 1977). This project aims to test the presence of contrast gain control mechanisms in the compound eyes of live horseshoe crabs. One would assume that the visual circuitry of the invertebrate is too simple to execute a complicated, multi-level mechanism such as contrast adaptation. Demonstrating a variance-dependent gain control process in the compound eye will challenge our current picture of retinal adaptation, and perhaps render it faulty.

CHAPTER 2: METHODS

2.1 Animals

The experiments were performed on male *Limulus polyphemus* from Marine Biological Laboratory (Woods Hole, MA). The eggs of the horseshoe crab are housed underneath the carapace of the female; therefore males were exclusively studied due to a simpler surgical isolation of the optic nerve. The animals were kept in an Oceanariums Seafood Holding System in tap water at 62° F with a specific gravity of 1.023-1.025. The salinity of the tank was adjusted using InstantOcean Salt. The crabs were retained in a 50 gallon tank on a 12 hour light cycle (9:00 AM-9:00 PM) via a 12V Arthograph LightPad A930. They were fed fresh clams every 10-12 days and roughly 20% of the tank was replaced with new water after every shipment.

2.2 Surgical Procedure

A horseshoe crab with clear eyes was selected for experimentation during the day cycle and 10 cm^3 of blood were extracted from the animal by inserting a 16 G needle through the hinge muscles into the heart and letting the blood drip into a beaker. This step is done to help control the bleeding during the surgical procedure. The horseshoe crab was then secured to a wooden platform fitted to a small water tank via metal screws inserted into

the front and middle section of the body and submerged to the gills in cold saltwater from the same tank that the crabs are held. This step was performed to help keep the animal comfortable for the duration of the experiment. The cornea was covered with modeling clay to shield the eye from the microscope light and a 2 cm hole was cut out of the carapace roughly 2 cm anterior to the lateral eye using a trephine and a scalpel. The optic nerve was cleaned of overlying connective tissue, exposed and guided into the tongue of a recording chamber by looping a piece of fabric thread around the nerve and using curved forceps to guide it through. The chamber is designed to fit securely in the 2 cm hole and the tongue is positioned to accommodate the nerve without pinching it. The nylon recording chamber was secured to the animal with two screws and cotton was applied on the sides to prevent blood and tissue from entering the chamber and clotting the nerve. If blood escapes through, the nerve could be starved of oxygen and yield unsuccessful recordings. The chamber was then filled with a Ringer's saline solution composed of 25.129 g/l NaCl, 0.713 g/l KCl, 1.399 g/l $CaCl_2 \cdot 2H_2O$, 2.027 g/l $MgCl_2 \cdot 6H_2O$, 5.188 g/l $MgSO_4 \cdot 7H_2O$, 0.11 g/l TES (50 mM), 0.012 g/l HEPES (50 mM) and 10 ml/l Penicillin-Streptomycin. The optic nerve was desheathed using straight Vanna micro- scissors and a single nerve fiber was carefully isolated and cut at distal end for afferent nerve recording. This procedure is performed under a stereoscope. The fiber was then directed into an A-M Systems suction electrode mounted to the

animal using a flexible fine probe. The tips of the electrode were made by flame polishing the end of 1 mm dia Borosilicate glass capillaries. A silver chloride wire serves as the reference and is wrapped around the electrode and glass capillary to help eliminate noise. A detailed description of the recording technique has been previously reported (Herzog *et al*., 1993).

2.3 Experimental Set-Up

The experimental set-up is shown in Figure 2.1. All experiments were conducted inside a light-tight recording booth within the laboratory. A 150 μm fiber optic was lined up with the visual axis of the recorded cell via a 5-dimentional micromanipulator. The precise position was determined by moving the light source slowly around the ommatidia and listening to the responsivity of the nerve fiber through speakers connected to the data acquisition system and confirming visually via an oscilloscope. The fiber optic was positioned right against the cornea and presented random stimulus at varying contrast (25%, 50%, 75% and 100%) and varying mean luminance (0.6 cd/m^2, 6 cd/m^2 and 60 cd/m^2, with and without background light) to ommatidia via a fiber optic light pipe coupled to a projector using the aluminum coupler shown in Figure 2.2. Whole eye illumination data was acquired by exchanging the 150 μm light pipe for a bigger one that has the ability to diffuse light over the whole eye and test the link between contrast adaptation and lateral inhibitory synapses.

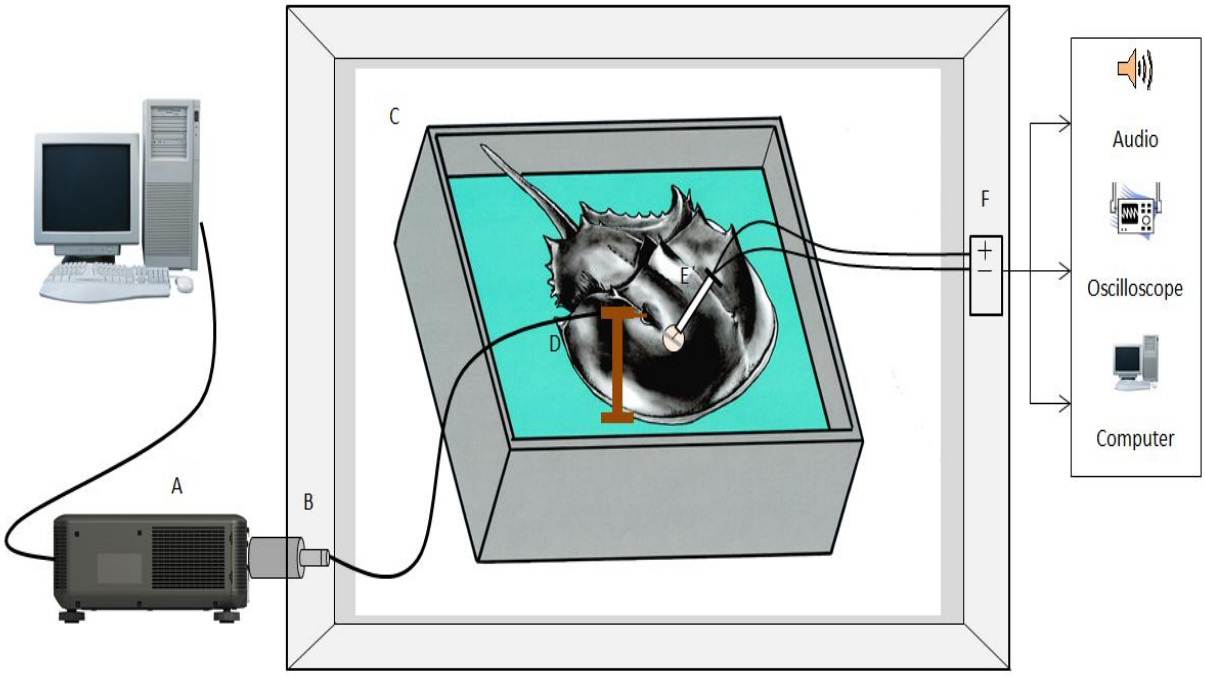

Figure 2.1 Experimental Set-up *A): Viewsonic 3,700 cd/m^2 projector controlled via a designated computer. B): Light coupler. C): Metal enclosure. D): Fiber optic light pipe stimulating recorded ommatidia. E): Suction electrode. F): FHC differential bioamplifier.*

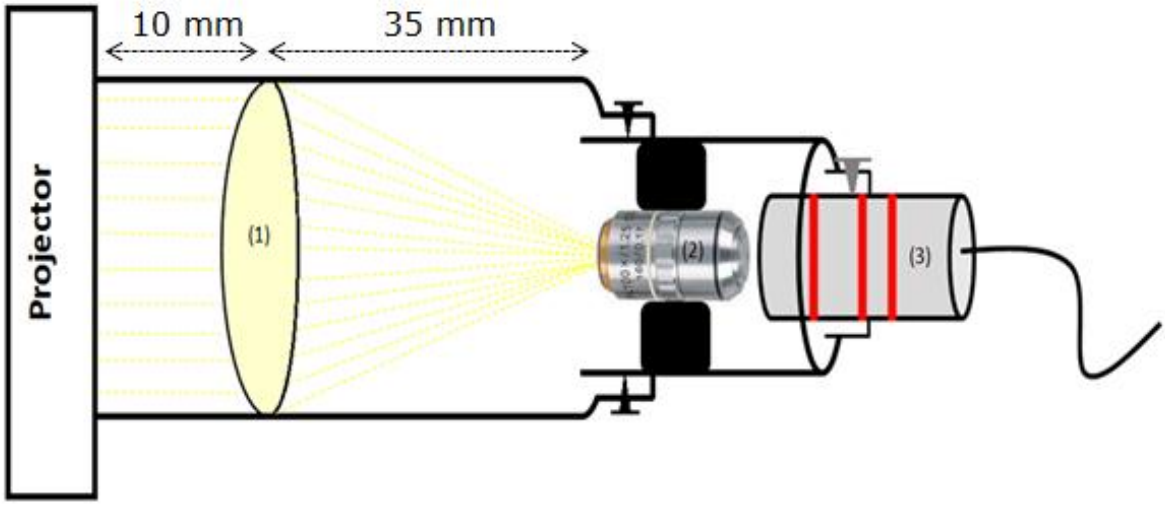

Figure 2.2 Fiber Optic Coupler *1). Edmund Optics 40 mm dia converging lens. 2): Spencer Microscope 45x objective lens. 3). Fiber optic light pipe.*

I custom designed the coupler to collimate and focus the light coming from a View Sonic projector to a fiber optic light, stimulating a single horseshoe crab ommatidia. The light stimulating system is unique in this ability. First, the projector output of 3,700 cd/m^2 is converged to a focus via an Edmund Optics uncoated plano-convex lens. The converging lens is 40 mm in diameter with a back focal length of 35.12 mm ± 1%, resulting in an output of ~ 680 cd/m^2. The focused light is then guided into a Spencer Microscope 45x magnifying lens. The 150 µm fiber optic light pipe input end is positioned a short distance away from the microscope lens. The brightness produced by the fiber optic is controlled between three settings (0.6 cd/m^2, 6 cd/m^2 and 60 cd/m^2) by moving the light coupler at precise and marked distances away from the magnifying lens. A set screw secures the position and ensures that a known brightness level is used at all times. Each stimulus was applied for a total of 120 seconds for each contrast condition. The experiments were performed inside a metal Faraday cage, preventing noise and ambient light coming from the projector from interfering with the signal. A fully computerized system presented the stimulus and recorded the nerve impulses. The micro-suction electrode leads were connected to a differential bio amplifier (FHC), which amplified the signal and filtered noise. The output of the amplifier was connected to an oscilloscope for signal visualization, a speaker for audio and a data acquisition card (National Instruments Inc., Austin, TX). The white noise stimulus was presented via a custom LabVIEW

program (Liu and Passaglia, Boston University), shown in Figure 2.3. A spike discriminator program (APM) was used to record the spike trains.

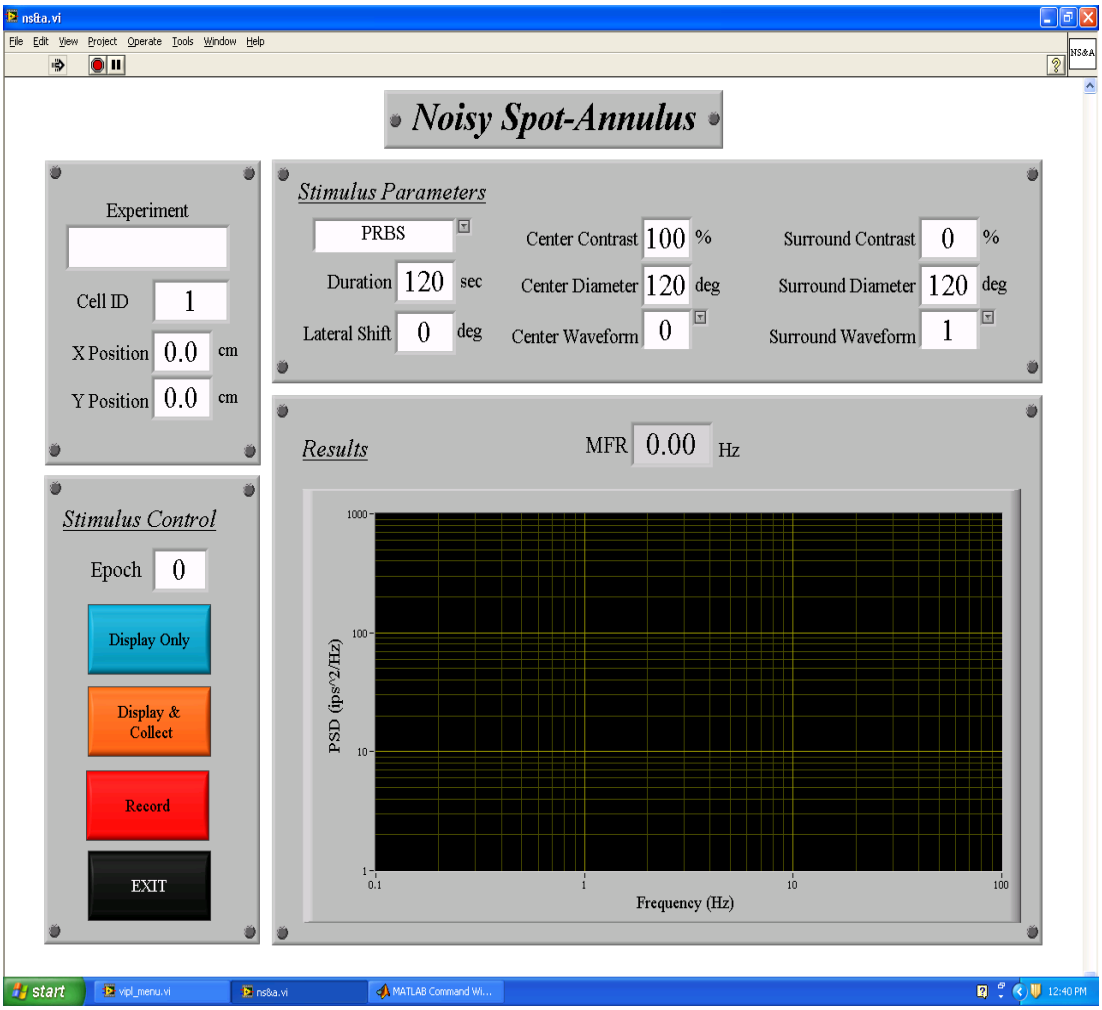

Figure 2.3 LabVIEW Program

2.4 LN Analysis

The nature of the adaptive mechanism and cell sensitivity in the retina was analyzed via linear-nonlinear (LN) cascade analysis of spike trains at each stimulus intensity level, Figure 2.4. An LN model provides a good characterization and quantification of the neural response, because it can be

used in spite of response nonlinearities (i.e. spike threshold and response saturation). The ganglion cell is mathematically modeled as a linear temporal filter, which is convolved with the stimulus, resulting in the spike-triggered average (STA) specifying which stimulus, on average, caused a spike in the cell (Chichilnisky, 2001; Zaghloul *et al*, 2005). The stimulus in this experiment is a pseudorandom binary sequence, which is a random time series of positive and negative steps of equal magnitude. The STA is inputted into a contrast-independent nonlinearity, accounting for rectification and saturation properties of the cell, completing the analysis and resulting in firing rate as a function of the stimulus. A detailed description of the linear-nonlinear analysis has been previously reported (Chichilnisky, 2001).

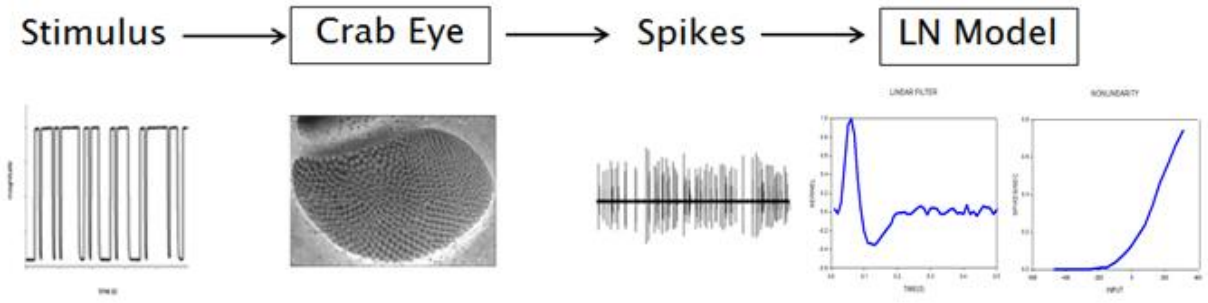

Figure 2.4 Linear-Nonlinear Cascade Analysis

For retinal ganglion cells, the cumulative normal density provides a good description of the nonlinear function. The function parameters were estimated by fitting the non-linear data for each condition to the indefinite integral of the normal distribution, Equation 1 (Chichilnisky, 2000):

$$f(x) = \alpha * e^{-0.5*((\frac{x-\gamma}{\beta})\text{^}2)} \quad (1)$$

where the parameters α, β and γ were selected to fit the graph with least squared error. Alpha is presumed to be the maximum firing rate of the cell, beta the sensitivity to the stimulus, and gamma the maintained drive of the cell in the absence of net visual stimulation (Chichilnisky, 2000). The phenomenological events for spike filter amplitude and duration were measured in the linear filter to evaluate occurrence of adaptation in synaptic inputs as well as in the process of spike generation. The MATLAB code is included in Appendix A.

2.5 Statistical Analysis

Analysis of variance (ANOVA) was used to analyze the difference and associated variance between the means for background/no background condition, contrast and mean illumination level variance for each cell. ANOVA is a useful tool for defining a significant change in means when more than two experimental conditions are compared simultaneously.

CHAPTER 3: RESULTS

Responses from a total of 25 individual cells were recorded and analyzed for 4 different contrast conditions (25, 50, 75 and 100%) and 3 different mean light levels (0.6, 6.0 and 60 cd/m^2), with and without background light. Whole-eye illumination data was acquired from 2 animals for 2 light conditions (30 and 840 cd/m^2). The waveform shape of the STA and the slope of the nonlinearity are evaluated for each light and contrast condition.

3.1 Effects of Light Level

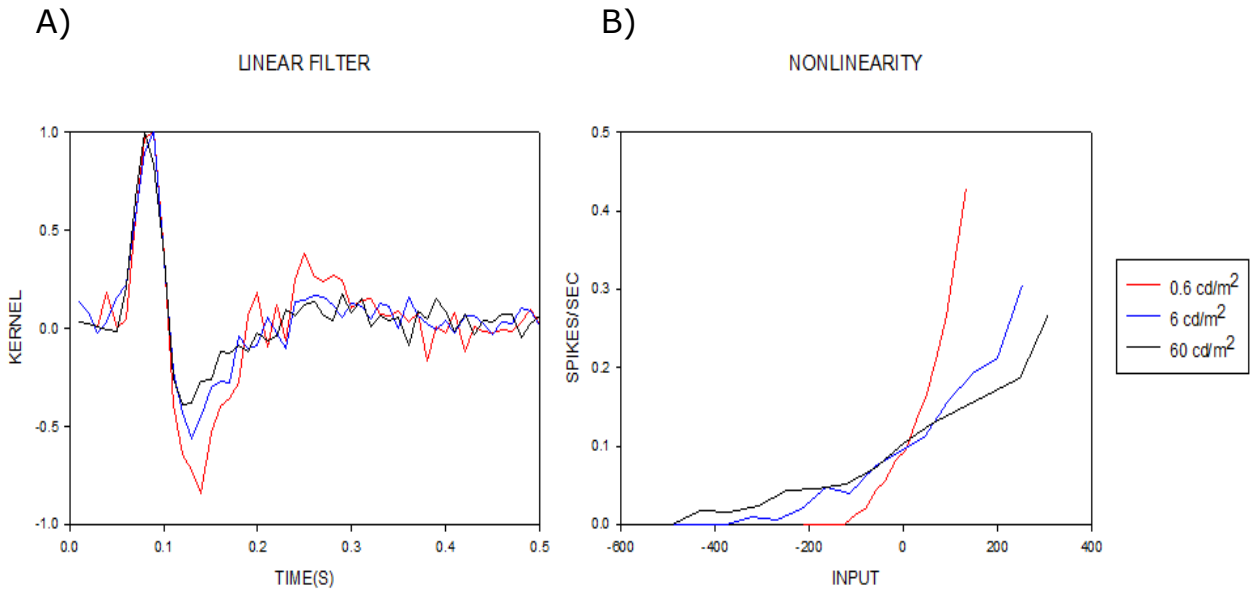

Figure 3.1 Effect of Light Level

Luminance adaptation is one of the image processing mechanisms known to exist in the invertebrate retina. Figure 3.1 is a summary plot of the effect on response with change in mean light level intensity. The linear filter waveform (Figure 3.1A) becomes less biphasic and the slope of the nonlinearity (Figure 3.1B) decreases with increasing illumination. The graphs show a clear decrease in gain, or sensitivity, of the cell with increasing stimulus intensity, exhibiting light adaptation.

3.2 Effects of Contrast

The summary results from the LN analysis of the data collected for each contrast condition are shown in Figure 3.2.

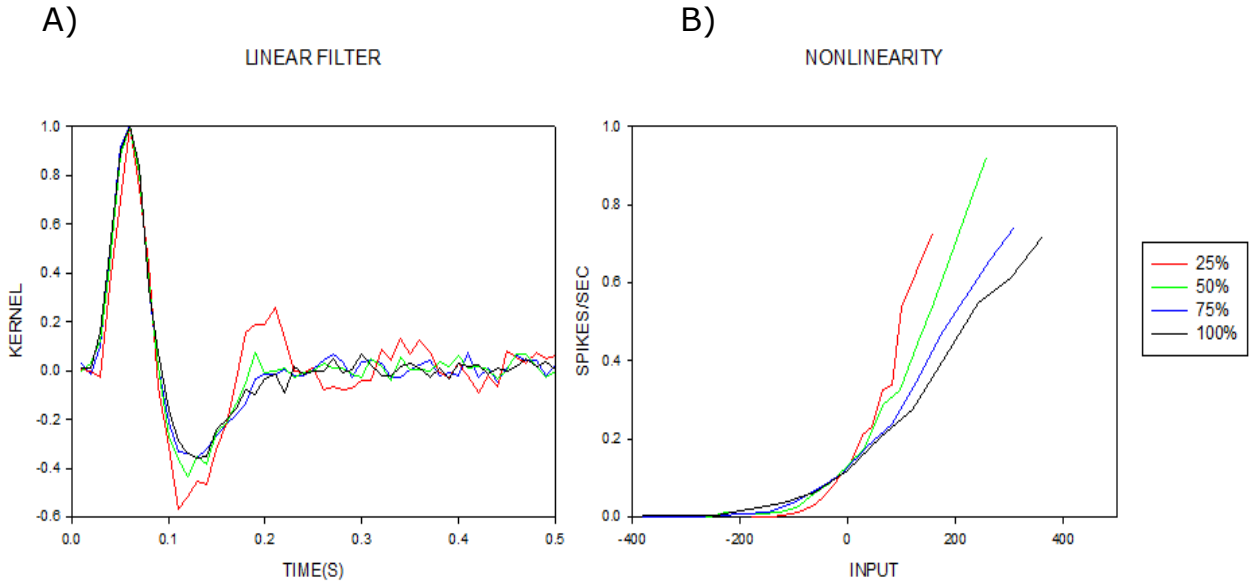

Figure 3.2 Effect of Contrast

The linear waveform amplitude and nonlinear gain decrease with increase in contrast, similar to the results found in the previous section.

3.2.1 Waveform Amplitude

The total change in amplitude of the linear waveform was evaluated for each contrast level and each light condition. The significance of introducing background light while recording from single cells is illustrated in Figure 3.3. The amplitude was normalized to the maximum contrast condition (100%), so inferences can be made about the overall relationship of waveform amplitude with the introduction of background light across experiments.

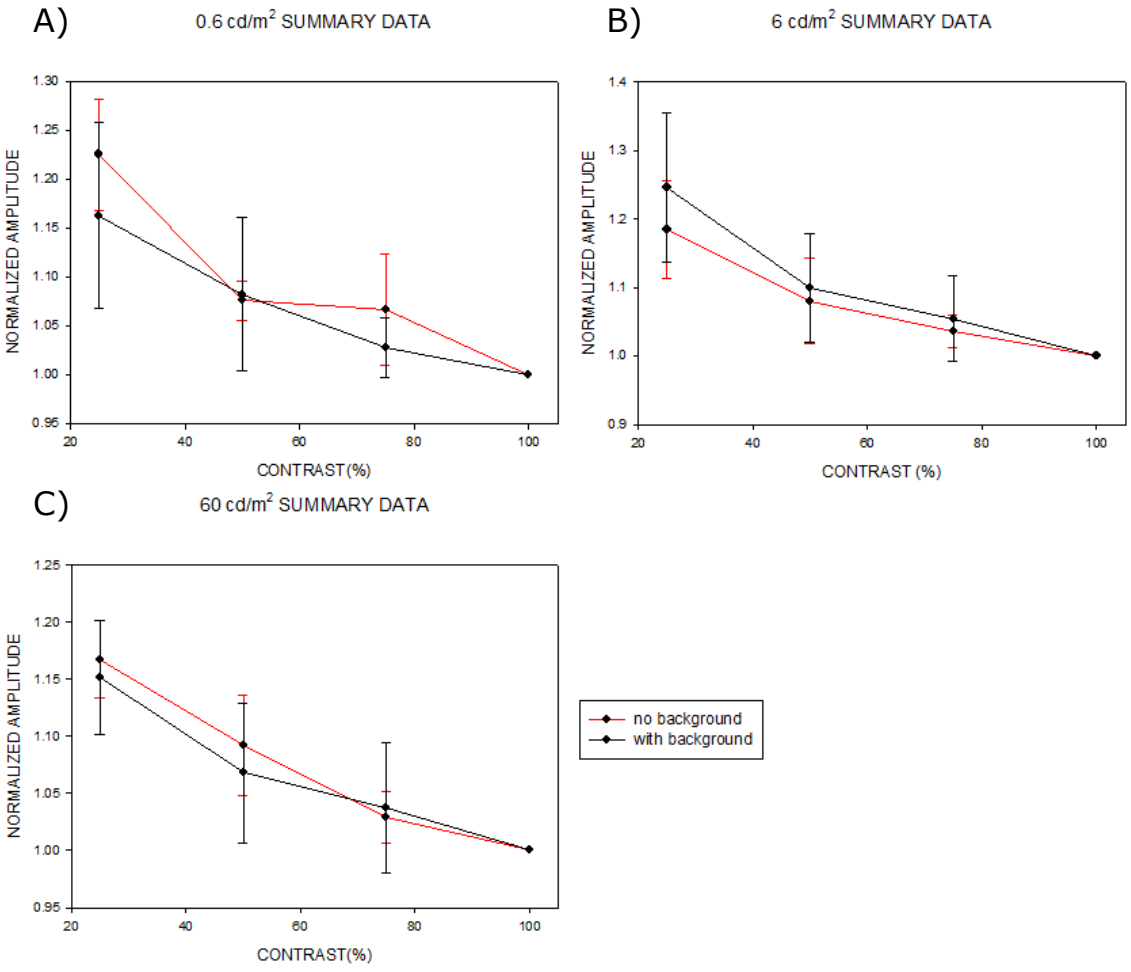

Figure 3.3 Background Effect on Waveform Amplitude

The summary from the statistical analysis of influence of background light on waveform amplitude for each mean luminance level is summarized in Table 3.1.

Table 3.1 Statistical Analysis of Effect of Background Addition on Waveform Amplitude

Light Level	*p.* val
0.6 cd/m^2	0.0975
6 cd/m^2	0.1079
60 cd/m^2	0.2248

There was no effect of background condition on the response. The data was combined irrespective of background for each light level, shown in Figure 3.4, and analyzed for effect on waveform amplitude with change in contrast as well as mean light level.

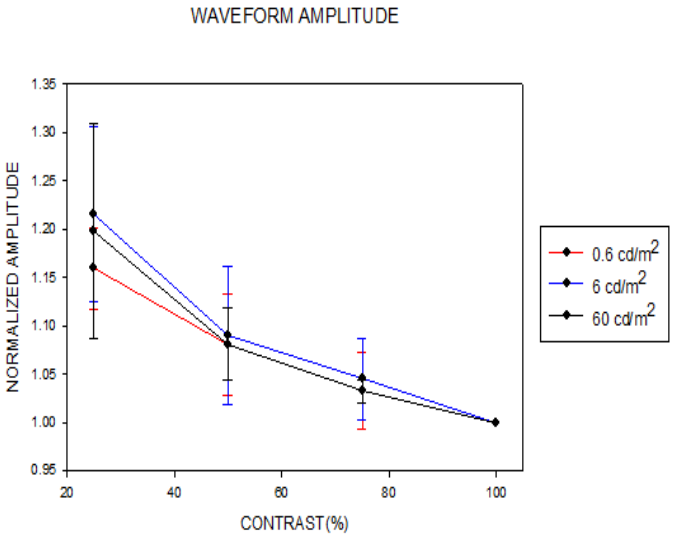

Figure 3.4 Waveform Amplitude Summary Data

There is a significant effect on sensitivity with change of contrast ($t(24)=-6.98$; $p=<0.0001$), but no effect on contrast adaptation with change

in stimulus intensity or illuminating whole eye vs. single cell (t(24)=0.4; *p*=0.6922). The raw data is included in Appendix B.

3.2.2 Nonlinearity Slope

Beta is the most important nonlinear parameter in studying the shape and slope of the nonlinearity as it relates to contrast adaptation and is akin to the sensitivity, or gain, of the cell. The effect on sensitivity with the introduction of background light while recording from single cells is illustrated in Figure 3.5.

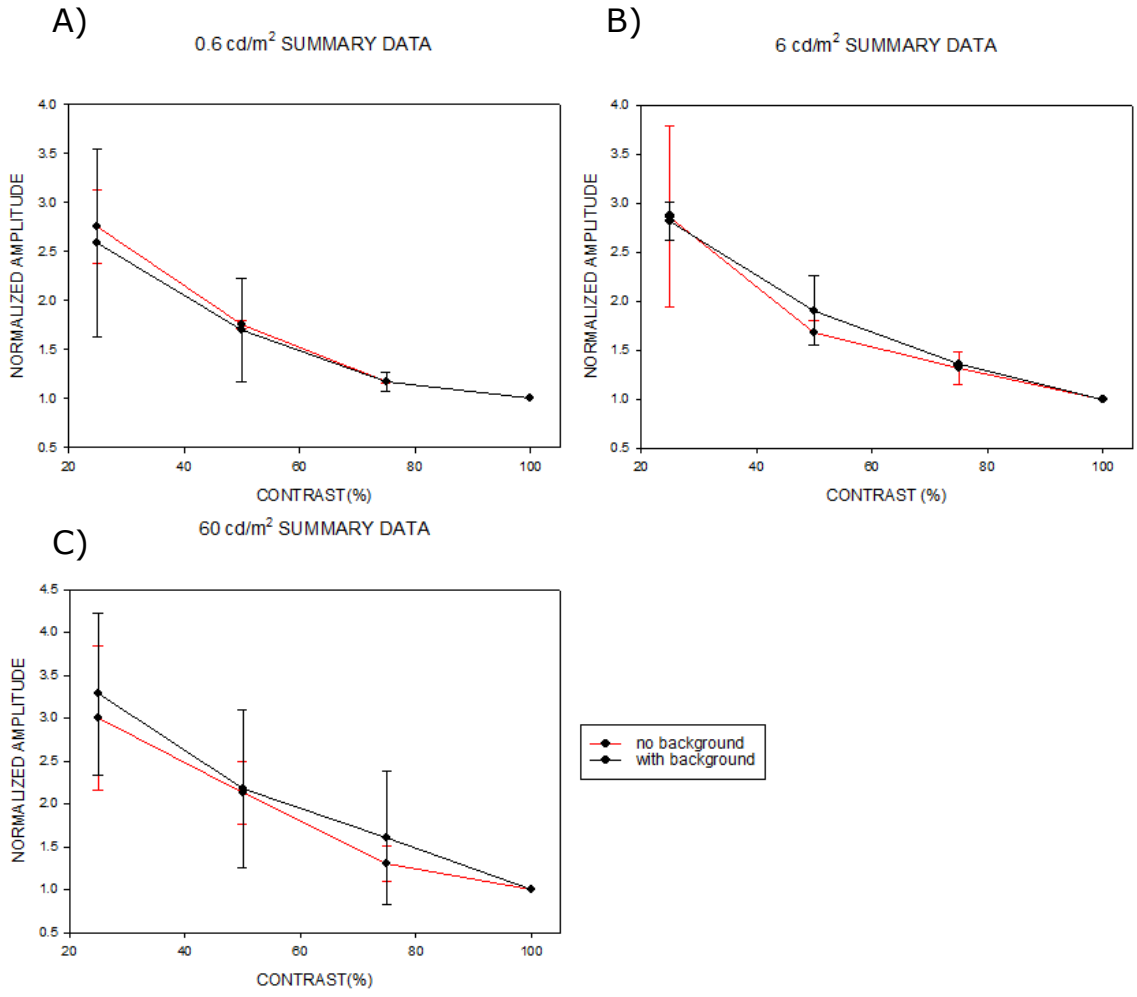

Figure 3.5 Background Effect on Sensitivity

Table 3.2 shows that there is no statistical difference in sensitivity with the addition of background light to the single cell illumination data. There is also no effect to a change in contrast with a decrease in whole eye illumination intensity (t(15)=1.26, *p*=0.2304).

Table 3.2 Statistical Analysis of Effect of Background Addition on Sensitivity

Light Level	*p.* val
0.6 cd/m^2	0.7449
6 cd/m^2	0.4401
60 cd/m^2	0.8411

Figure 3.6 shows the summary data for the sensitivity of the cells with change in contrast. There is a significant effect on gain with change of contrast (t(24)=4.05; *p*=<0.0001), but no effect on contrast adaptation with change in stimulus intensity or illuminating whole eye vs. single cell (t(24)=-0.61; *p*=0.5435).

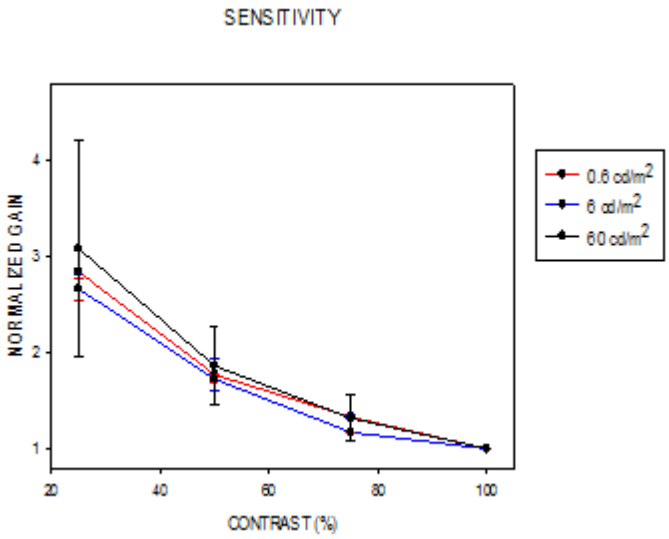

Figure 3.6 Sensitivity Summary Data

3.3 Supplemental Data

There was no statistical effect of background on the linear filter duration (Table 3.3), as well as no effect on response to change in contrast with change in whole eye illumination intensity ($t(15)=0.51$, $p=0.6119$). There was also no effect on duration with changing contrast conditions ($t(24)= 0.62$; $p=0.5345$), as well as no effect with change in stimulus intensity or illuminating whole eye vs. single cell ($t(24)=0.63$; $p=0.5325$).

Table 3.3 Statistical Analysis of Effect of Background Addition on Waveform Duration

Light Level	*p.* val
0.6 cd/m^2	0.6722
6 cd/m^2	0.9430
60 cd/m^2	0.9516

Alpha is akin to the maximum firing rate of the cell. Table 3.4 shows that there is no statistical difference in alpha with the addition of background light.

Table 3.4 Statistical Analysis of Effect of Background Addition on Alpha

Light Level	*p.* val
0.6 cd/m^2	0.0905
6 cd/m^2	0.2523
60 cd/m^2	0.1558

There is no effect to a change in contrast of the parameter with change in whole eye illumination intensity ($t(15)=-0.91$, $p=0.3802$). There was also no effect on alpha with changing contrast conditions ($t(24)=-1.92$;

p=0.0572), as well as no effect on alpha with change in stimulus intensity or illuminating whole eye vs. single cell (t(24)=-0.81; *p*=0.4219).

Gamma is akin to the maintained cell drive in the absence of a stimulus. Table 3.5 summarizes the statistical effects of adding background light while recording from a single fiber optic. There is no statistical significance in this parameter with the addition of background light or to a change in whole eye illumination intensity (t(15)=-0.42, *p*=0.6796).

Table 3.5 Statistical Analysis of Effect of Background Addition on Gamma

Light Level	*p.* val
0.6 cd/m^2	0.1735
6 cd/m^2	0.9452
60 cd/m^2	0.5426

There is a significant effect on gamma with change of contrast (t(24)=4.84; *p*=<0.0001), but no effect with change in stimulus intensity or illuminating whole eye vs. single cell (t(24)=-1.69; *p*=0.0952). Raw data for app supplemental parameters is included in Appendix B.

CHAPTER 4: DISCUSSION

The horseshoe crab eye is thought of as a simple, fairly linear system at a given light level. Luminance adaptation is the only gain control mechanism that is known to occur in the *Limulus* eye to date. The experimental data for mean light level follows longstanding dogma about light adaptation in the invertebrate eye (Figure 3.1). This validates our model and methods for quantifying contrast adaptation in the retina of live horseshoe crabs. Without any adaptation to change in light stimulus, the linear waveform shape and the slope of the nonlinear filter would remain the same through change in stimulus conditions, exemplified in Figure 4.1.

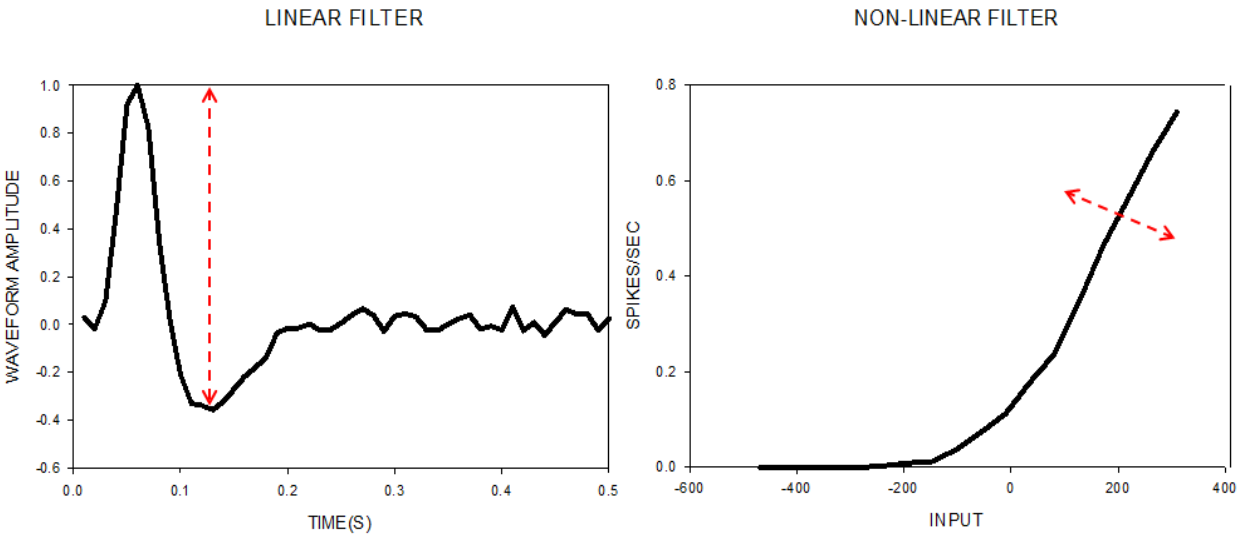

Figure 4.1 No Adaptive Mechanism

LN analysis suggests that an unknown contrast adaptation phenomenon might operate in the invertebrate retina, resting on the assumption that retinal processing can be sufficiently described by an LN model (Figure 3.2). There is a clear decrease in STA waveform amplitude and gain with increase in contrast (Figure 3.4 and Figure 3.6), signifying the existence of a contrast gain control mechanism in the eye. This questions our current picture of retinal adaptation and perhaps renders it wrong.

There is no change in STA duration or nonlinear parameter alpha with change in contrast. There was a change in the last nonlinear parameter, gamma, with a change in contrast. Gamma is representative of the cell drive in the absence of a stimulus. The results show that the cell drive increases with an increase in intensity.

The next step is to determine where in the *Limulus* visual hierarchy contrast adaptation occurs via intracellular recordings of the voltage fluctuations of single cell membranes evoked by the stimulus. By showing that the relatively simple eye of the invertebrate can accomplish the same task as the intricate, multi-layer vertebrate retina, we can narrow down the key players behind contrast adaptation. The experimental results show no effect on contrast adaptation with the introduction of background light as well as no effect in sensitivity with whole eye vs. single cell illumination. This means that the gain control mechanism is unlikely to occur in the inhibition cascade.

A computational model that accurately predicts the output of the *Limulus* eye to underwater visual scenes using a contrast gain control mechanism does not show contrast adaptation. The validity of the assumption that the retinal processing of *Limulus* can be sufficiently described by an LN model with contrast gain control needs further investigation as a more complex and realistic model of the eye does not exhibit contrast adaptation to white noise stimulation.

A complete understanding of light and contrast adaptation is currently lacking and consequently of fundamental importance in vision research. It is central to understand the mechanisms of the visual system to aid in disease diagnosis, treatment and prevention as well as make advancements in the development of ocular assisting devices. If we know exactly how the eye converts and transmits signal to the brain, engineers can develop ocular assisting devices that will be able to convey information in a similar manner and improve the quality of life of those whose eyes cannot be saved.

REFERENCES

Baccus, S.A. and Meister, M., "Fast and slow contrast adaptation in retinal circuitry", *Neuron*, vol. 36., pp. 909-919, 2002.

Barlow, R.B., Hitt, J.M. and Dodge, F.A., "*Limulus* Vision in the Marine Environment",*Biol. Bull*., vol. 200, no.2, pp. 169-176,2001.

Berry, M.J., Brivanlou, I.H., Jordan, T.A. and Meister, M., "Anticipation of moving stimuli by the retina",*Nature*, vol. 398, pp. 334-338, PMID: 10192333, 1999.

Berson, D.M., Dunn, F.A. and Takao, M., "Phototransduction by retinal ganglion cells that set the circadian clock", *Science,* vol. 295, pp. 1070-103., PMID: 11834835, 2002

Bonin, V., Mante, V. and Carandini, M., "The suppressive field of neurons in lateral geniculate nucleus", *J Neurosci.*, vol. 25, pp.10844-10856, PMID: 16306397, 2005.

Chandler, D. and Chichilnisky E.J., "Adaptation to temporal contrast in primate and salamander retina", *J Neuroscience*, vol. 25, pp. 9904-9916, 2001.

Chichilnisky, E.J., "A simple white noise analysis of neuronal lightresponses", Network, vol. 12, pp. 199–213, 2001.

Demb, J.B., "Functional circuitry of visual adaptation in the retina", *J. Physiol*., vol. 586, pp. 4377–4384, 2008.

Downling, J.E., " The Retina- An Approachable Part of the Brain". Harvard Univ. Press, Cambridge, Massachusetts, 1987.

Dyer, M.A. and Cepko, C.L., "Regulating proliferation during retinal development", *Nature Reviews Neuroscience*, vol. 2, pp. 333-342, 2001.

Green, D.G., Tong, L. and Cicerone, C.M., "Lateral spread of light adaptation in the rat retina", *Vision Res.*, vol.17, pp. 479-486, PMID: 878339, 1977.

Herzog, E. D., Powers, M. K. and Barlow, R. B., "*Limulus* vision in the ocean day and night: effects of image size and contrast". *Visual Neuroscience*, vol.13, pp. 31-41, 1996.

Kim, K.J. and Rieke,F., "Temporal Contrast Adaptation in the Input and Output Signals of Salamander Retinal Ganglion Cells", *J. Neuroscience*., vol. 21, pp. 287-299, 2001.

Knight, B.W, Toyoda, J. and Dodge, F.A., "A Quantitative Description of the Dynamics of Excitation and Inhibition in the Eye of *Limulus*", *J. of Gen. Physiol.,* vol. 56, pp. 421-437, 1970.

Laughlin, S.B., "The Role of Sensory Adaptation in the Retina", *J. Exp.Biol*., vol. 146, pp. 39-62, 1989.

Le, N.,"Computational Systems Neurobiology."Dordrecht:Springer,pp. 300 315, 2012.

Liu, J.S. and Passaglia, C.L., "Using the horseshoe crab, *Limulus polyphemus* in vision research" *J. Vis. Exp*., vol. 29, pp. 1384, doi: 10.3791/1384, 2009.

Lund, A. and Lund, M., "Dependent T-Test for Paired Samples", *Dependent T-Test*. Lund Research Ltd, 2013. Web. 01 Oct. 2013. <https://statistics.laerd.com/>.

Mante,V., Frazor, R.A., Bonin, V., Geisler, W.S. and Carandini,M., "Independence of luminance and contrast in natural scenes and in the early visual system", *Nat. Neurosci.,* vol. 8, pp. 1690-7,2005.

Passaglia, C.L., Dodge, F.A. and Barlow, R.B., "A cell-based model of the *Limulus* lateral eye", *J. Neurophysiol*., vol. 80, pp. 1800-1815, 1998.

Passaglia, C.L., Dodge, F.A., Herzog, E.D., Jackson, S.A. and Barlow,R.B., "Deciphering a neural code for vision", Proc. Natl. Acad. Sci., vol. 94, pp. 12649-54, 1997.

Purpura, K., Tranchina, D., Kaplan, E. and Shapley, R.M., "Light adaptation in the primate retina: Analysis of changes in gain and dynamics of monkey retinal ganglion cells", *Visual Neuroscience*, vol. 4, pp. 75-93, 1990.

Roska, B., Nemeth, E., Orzo, L. and Werblin, F. S., "Thre levels of lateral inhibition: A space-time study of the retina of the tiger salamander", *J Neuroscience,* vol. 20, pp. 1941-1951, 2000.

Shapley, R. M. and Enroth-Cugell, C., "Visual adaptation and retinal gain controls", Prog. Retinal Res., vol. 3, pp. 263-346, 1984.

Tamura, T., Nakatani, K. and Yau, K.W., "Light adaptation in cat retinal rods", *Science*, vol 245, no. 4919, pp. 755-758, 1989.

Thalheimer, W. and Cook,S., "How to calculate effect sizes from published research articles: A simplified methodology*"*, 2002.Retrieved September 26, 2013 from http://worklearning.com/effect_sizes.htm

Tranchina, D., Gordon, J. and Shapley, R.M., "Retinal light adaptation-evidence for a feedback mechanism", *Nature*, vol. 310, pp. 314-316, 1984.

Valtcheva, T.M. and Passaglia, C.L., "Adaptive Processes of the *Limulus* Lateral Eye" SBEC, vol. 29, pp. 51-52, 2013.

Van, B. G. and Fisher, L.,"Biostatistics: A Methodology for the Health Sciences. Hoboken", NJ: John Wiley & Sons, 2004.

Wald, G. and Krainin, J. M., "The median eye of *Limulus*: an ultraviolet receptor. *PNAS* vol.50(6), pp. 1011-1017, 1963.

Yu, Y. and Lee, T.S., "Dynamical mechanisms underlying contrast gain control in single neurons", *Phys Rev E Stat Nonlin Soft Matter Phys,* vol. 68, 011901, 2003.

Zaghloul, K.A., Boahen, K. and Demb, J.B., "Contrast adaptation in subthreshold and spiking responses of mammalian Y-type retinal ganglion cells', *J. Neuroscience*, vol. 23, pp. 2645-2654, 2005.

Zaghloul, K.A., Manookin, M.B., Borghuis, B.G., Boahen, K. and Demb, J.B., "Functional circuitry for peripheral suppression in mammalian Y-type retinal ganglion cells', *J. Neurophysiology*, vol. 97, pp. 4327-4340, 2007.

APPENDICES

Appendix A. MATLAB Codes

LN analysis for analysizng spike trains from live horseshoe crabs is below.

```
function [t,s,r,tsta,sta,bin,cnt] = lnmodel(duration,frate,conts,spikes)
% [t,s,r,tsta,sta,bin,cnt] = lnmodel(duration,frate,conts,spk)
% Computes linear-nonlinear model of spike response
%
%Written by: Christopher Passaglia, 2012
%Edited by: Tchoudomira Valtcheva, 2012

load('C:\Users\tvaltche\Documents\Data\L9\C1E18.mat')
if ~exist('duration'), duration=180; end;
if ~exist('frate'), frate=100; end;
if ~exist('conts'), conts=20; end;

% define time base
upsample = 1;
srate = frate*upsample;
t = (0:1/srate:duration-1/srate)';

% get stimulus
load 'C:\Users\tvaltche\Documents\prbs\prbs0.mat';
for x=1:duration*frate,
    s(upsample*(x-1)+1:upsample*x,1)=conts*(2*prbs(1,x)-1)*ones(upsample,1);
end;
r(:,1)=histc(spikes,t);

% determine spike triggered average
Nsta = floor(srate);
tsta = (1/srate:1/srate:Nsta/srate)';
sta = zeros(Nsta,1);
ind = find(r); ind = ind(find(ind>Nsta));
for n=1:length(ind), sta = sta + s(ind(n)-Nsta:ind(n)-1,1); end;
sta = flipud(sta)/sum(r(ind));
sta = sta/max(abs(sta));

% map nonlinearity
Nbin = 21;
g = conv(sta,s); g = g(1:length(s),1);
bin = linspace(min(g),max(g),Nbin);
cnt = zeros(Nbin,1);
for n=1:Nbin-1,
    ind = find(g>=bin(n) & g<bin(n+1));
    cnt(n,1) = sum(r(ind))/sum(ind);
end;
bin=bin';
cnt=srate*duration*cnt;
% plot results
figure(1)
plot(tsta,sta)
figure(2)
plot(bin,cnt)
```

Appendix A. (Continued)

Raster plot and mean firing rate MATLab code is below.

```
%Written by: Christopher Passaglia, 2012
%Edited by: Tchoudomira Valtcheva, 2012

load('C:\Users\tvaltche\Documents\Data\L9\C1E12.mat')
 times=spikes';
 period=5.12;

 if ~exist('times'), error('No spike train!'), end;
 if ~exist('period'), period=1; end;
 % epoch is the time that the last spike occurred at
 epoch=times(max(find(times(:,1)>0)),1);
  % N is the number of trials
  N=ceil(epoch/period);
  for n=1:N,
      % t divides the total time into trial periods and runs them a trial
      % at a time
      t=(n-1)*period;
      % x is the number of spikes in the trial n
      x=find(times(:,1)>t & times(:,1)<t+period);
      % rtimes are the spike times for trial n
      rtimes(1:length(x),n)=times(x,1)-t;
      end;
       X = []; Y =[];
       for n = 1:N
           x=rtimes(:,n); y = n*ones(length(x),1);
           X = [X;x]; Y = [Y;y];
       end
       %raster plot
           hold on
           figure(1)
           scatter(X,Y,3, 'fill')
           axis([0 5.13 0 70.5])
           title ('L9 CW 7')
           ylabel('trial #')
           hold off
       %mean firing rate
           nbins=period/0.01;
           hold on
           figure(2)
           hist(X,nbins)
           xlabel('time(s)')
           ylabel('mean firing rate')
           axis([0 5.13 0 45])
           hold off
```

Appendix B. Raw Data

Table B.1 Linear Filter Amplitude Raw Data

Condition	25% contrast	50% contrast	75% contrast	100% contrast
0.6 cd/m^2	1.363	1.254	1.18	1.15
0.6 cd/m^2	1.342	1.308	1.235	1.22
0.6 cd/m^2	1.44	1.328	1.196	1.119
0.6 cd/m^2	1.43	1.2	1.25	1.13
0.6 cd/m^2	1.341	1.275	1.214	1.217
0.6 cd/m^2	1.5	1.399	1.418	1.393
6 cd/m^2	1.44	1.313	1.319	1.266
6 cd/m^2	1.389	1.38	1.278	1.239
6 cd/m^2	1.368	1.275	1.262	1.23
6 cd/m^2	1.66	1.303	1.294	1.285
6 cd/m^2	1.642	1.396	1.308	1.297
6 cd/m^2	1.839	1.625	1.56	1.387
6 cd/m^2	1.712	1.64	1.493	1.403
60 cd/m^2	1.566	1.436	1.358	1.351
60 cd/m^2	1.29	1.207	1.169	1.119
60 cd/m^2	1.254	1.209	1.173	1.103
60 cd/m^2	1.387	1.265	1.184	1.148
60 cd/m^2	1.493	1.442	1.26	1.232
60 cd/m^2	1.339	1.281	1.346	1.267
60 cd/m^2	1.485	1.254	1.149	1.182
60 cd/m^2	1.268	1.257	1.197	1.11
60 cd/m^2	1.44	1.45	1.4	1.39
Whole Eye	1.378	1.296	1.28	1.26
Whole Eye	1.419	1.371	1.291	1.24
Whole Eye	1.638	1.32	1.237	1.19
Whole Eye	1.56	1.43	1.27	1.39

Appendix B. (Continued)

Table B.2 Linear Filter Duration Raw Data

Condition	25% contrast	50% contrast	75% contrast	100% contrast
0.6 cd/m^2	0.14	0.13	0.13	0.14
0.6 cd/m^2	0.15	0.14	0.14	0.15
0.6 cd/m^2	0.1	0.12	0.1	0.09
0.6 cd/m^2	0.15	0.13	0.14	0.14
0.6 cd/m^2	0.07	0.08	0.07	0.08
0.6 cd/m^2	0.09	0.09	0.1	0.1
6 cd/m^2	0.05	0.04	0.04	0.04
6 cd/m^2	0.05	0.05	0.05	0.06
6 cd/m^2	0.1	0.11	0.11	0.12
6 cd/m^2	0.1	0.11	0.11	0.11
6 cd/m^2	0.11	0.1	0.11	0.11
6 cd/m^2	0.11	0.1	0.13	0.1
6 cd/m^2	0.07	0.07	0.06	0.07
60 cd/m^2	0.07	0.06	0.07	0.07
60 cd/m^2	0.06	0.08	0.08	0.08
60 cd/m^2	0.06	0.07	0.07	0.08
60 cd/m^2	0.11	0.09	0.14	0.15
60 cd/m^2	0.07	0.11	0.1	0.1
60 cd/m^2	0.15	0.15	0.14	0.14
60 cd/m^2	0.14	0.14	0.15	0.15
60 cd/m^2	0.11	0.09	0.1	0.09
60 cd/m^2	0.07	0.06	0.05	0.07
Whole Eye	0.1	0.11	0.09	0.09
Whole Eye	0.13	0.13	0.14	0.13
Whole Eye	0.07	0.08	0.08	0.1
Whole Eye	0.05	0.05	0.06	0.05

Appendix B. (Continued)

Table B.3 Alpha Raw Data

Condition	25% contrast	50% contrast	75% contrast	100% contrast
0.6 cd/m^2	0.6881	0.5792	0.6655	0.572
0.6 cd/m^2	0.5396	0.5564	1.0826	1.0516
0.6 cd/m^2	1.3713	0.504	0.4293	0.2551
0.6 cd/m^2	0.0875	0.1791	0.2011	0.2167
0.6 cd/m^2	0.4637	0.8507	0.395	0.3575
0.6 cd/m^2	0.5298	0.6134	0.4889	0.4808
6 cd/m^2	0.6807	0.5612	0.5709	0.542
6 cd/m^2	0.2759	0.4752	0.4198	0.4374
6 cd/m^2	9.07749	0.4513	0.4695	0.7033
6 cd/m^2	0.304	0.3253	0.0298	0.7215
6 cd/m^2	0.2678	0.6498	0.3446	0.4736
6 cd/m^2	2.0114	0.6249	0.9599	0.7224
6 cd/m^2	7.40109	0.4182	0.3166	0.6131
60 cd/m^2	0.8666	1.1709	0.7859	0.7363
60 cd/m^2	0.541	0.6189	1.5651	1.2157
60 cd/m^2	1.1629	1.0739	3.4872	2.3134
60 cd/m^2	0.6172	0.7871	0.7788	0.3376
60 cd/m^2	0.2911	0.5291	0.8814	0.4925
60 cd/m^2	0.337	0.2907	0.1942	0.1783
60 cd/m^2	0.4755	0.3717	0.2526	3.0111
60 cd/m^2	0.3745	0.4394	0.3279	0.3044
60 cd/m^2	0.3784	0.3099	0.3239	0.7125
Whole Eye	0.3152	0.3796	0.4151	0.5702
Whole Eye	8.4535	1.1313	0.12	0.123
Whole Eye	0.7324	0.4812	0.3336	0.3139
Whole Eye	0.1795	0.2158	0.2283	0.2237

Appendix B. (Continued)

Table B.4 Beta Raw Data

Condition	25% contrast	50% contrast	75% contrast	100% contrast
0.6 cd/m^2	4.73E-03	3.74E-03	3.13E-03	2.48E-03
0.6 cd/m^2	5.08E-03	3.14E-03	2.53E-03	2.17E-03
0.6 cd/m^2	6.28E-03	4.05E-03	3.09E-03	2.99E-03
0.6 cd/m^2	6.29E-03	3.73E-03	2.42E-03	2.09E-03
0.6 cd/m^2	7.73E-03	5.36E-03	3.68E-03	3.11E-03
0.6 cd/m^2	1.03E-02	6.39E-03	3.17E-03	2.58E-03
6 cd/m^2	5.49E-03	4.04E-03	2.48E-03	1.83E-03
6 cd/m^2	8.62E-03	3.79E-03	2.97E-03	2.13E-03
6 cd/m^2	3.06E-03	6.37E-03	3.97E-03	2.86E-03
6 cd/m^2	5.89E-03	3.39E-03	2.86E-03	1.91E-03
6 cd/m^2	5.33E-03	4.08E-03	2.76E-03	2.05E-03
6 cd/m^2	3.08E-03	5.12E-03	4.68E-03	4.42E-03
6 cd/m^2	6.98E-03	3.69E-03	3.30E-03	2.44E-03
60 cd/m^2	8.91E-03	5.45E-03	5.11E-03	4.51E-03
60 cd/m^2	9.15E-03	5.56E-03	2.94E-03	2.20E-03
60 cd/m^2	3.35E-03	3.19E-03	1.95E-03	1.72E-03
60 cd/m^2	6.88E-03	4.14E-03	2.93E-03	2.55E-03
60 cd/m^2	2.38E-03	1.60E-03	1.11E-03	6.79E-04
60 cd/m^2	5.97E-03	4.07E-03	2.76E-03	2.12E-03
60 cd/m^2	5.70E-03	4.16E-03	3.25E-03	1.30E-03
60 cd/m^2	7.62E-03	4.05E-03	2.93E-03	2.87E-03
60 cd/m^2	5.53E-03	4.62E-03	2.50E-03	2.03E-03
Whole Eye	0.0124	6.26E-03	4.43E-03	2.68E-03
Whole Eye	5.50E-03	4.23E-03	3.76E-03	2.81E-03
Whole Eye	7.74E-03	4.27E-03	3.17E-03	2.77E-03
Whole Eye	8.10E-03	5.65E-03	3.09E-03	2.72E-03

Appendix B. (Continued)

Table B.5 Gamma Raw Data

Condition	25% contrast	50% contrast	75% contrast	100% contrast
0.6 cd/m^2	315.3223	428.5712	444.205	566.3764
0.6 cd/m^2	345.1415	660.3367	484.0439	745.9646
0.6 cd/m^2	553.1728	430.94	520.3729	428.1861
0.6 cd/m^2	102.8986	387.948	638.9778	785.4712
0.6 cd/m^2	201.5727	253.4973	439.0244	296.5704
0.6 cd/m^2	137.9679	223.6024	601.8011	777.8529
6 cd/m^2	455.2534	487.2536	872.7903	1099.9864
6 cd/m^2	1111.621	485.1591	560.8449	971.8415
6 cd/m^2	189.6387	518.5241	490.5167	839.4856
6 cd/m^2	180.2009	448.2134	468.737	658.5004
6 cd/m^2	1464.0841	235.5994	396.4656	769.2712
6 cd/m^2	239.8867	241.2884	303.6096	359.2961
6 cd/m^2	455.2534	487.2536	872.7903	1099.9864
60 cd/m^2	221.9429	384.4466	377.5876	422.2977
60 cd/m^2	185.8603	270.3561	717.7519	838.0781
60 cd/m^2	662.7591	696.4442	1402.254	635.7211
60 cd/m^2	293.1357	526.7143	852.2375	610.7447
60 cd/m^2	119.4769	402.2888	831.9577	2073.9765
60 cd/m^2	338.6545	500.8082	687.3603	919.9982
60 cd/m^2	423.2164	410.9059	566.3542	2415.6251
60 cd/m^2	196.1305	412.9451	510.0655	491.5526
60 cd/m^2	282.4204	336.1349	749.5633	1017.8614
Whole Eye	92.3176	216.5978	319.477	648.7441
Whole Eye	718.4799	612.6092	166.0439	144.7839
Whole Eye	217.5368	396.4079	457.7214	487.709
Whole Eye	185.338	267.0176	505.6281	585.6228

Appendix C. Copyright Permission for Figure 1.4

JOHN WILEY AND SONS LICENSE TERMS AND CONDITIONS

Oct 10, 2013

This is a License Agreement between Choko Valtcheva ("You") and John Wiley and Sons ("John Wiley and Sons") provided by Copyright Clearance Center ("CCC"). The license consists of your order details, the terms and conditions provided by John Wiley and Sons, and the payment terms and conditions.

All payments must be made in full to CCC. For payment instructions, please see information listed at the bottom of this form.

License Number	3245390689510
License date	Oct 10, 2013
Licensed content publisher	John Wiley and Sons
Licensed content publication	Journal of Physiology
Licensed content title	Functional circuitry of visual adaptation in the retina
Licensed copyright line	© 2008 The Author. Journal compilation © 2008 The Physiological Society
Licensed content author	Jonathan B. Demb
Licensed content date	Sep 15, 2008
Start page	4377
End page	4384
Type of use	Dissertation/Thesis
Requestor type	University/Academic
Format	Print and electronic
Portion	Figure/table
Number of figures/tables	1
Original Wiley figure/table number(s)	Figure 1
Will you be translating?	No
Total	0.00 USD